Parametric instability of LCGT interferometer

Kazuhiro Yamamoto
Albert Einstein Institute Hannover

October 24, 2009

1 Introduction

Parametric instability is one of the important issues in future interferometric detectors [1]. Such interferometers have at least a few km length arm cavities. The intervals of the optical modes in these long cavities are on the order of 10 kHz. This value is comparable with the intervals of elastic modes of mirrors of cavities. In such cases, the parametric instability becomes a serious problem in the stable operation of interferometers. Small thermally driven elastic vibration modulates the light and excites the transverse modes of the cavity. This excited optical modes apply modulated radiation pressure on the mirrors. This makes the amplitude of the elastic modes larger. At last, the elastic modes and optical modes, except for TEM00, oscillate largely. This is the parametric instability.

The parametric instability of a LCGT [2] arm cavity has already been discussed [3]. However, some work is remained as follows.

- Effect of PR (power recycling) and RSE (resonant sideband extraction)
- Instability suppression with PR and RSE
- Contribution of higher elastic and optical modes
- Contribution of anti-Stokes modes

In this report, the first two items are mainly discussed. The other items are also considered briefly.

2 Parametric instability of a LCGT arm cavity

Here the parametric instability of a LCGT arm cavity are summarized [3]. Table 1 gives the specifications of Advanced LIGO in Refs. [4, 5, 6] (after these references, the specifications of Advanced LIGO were changed slightly) and LCGT [2] (the exact values of the LCGT

mirror curvature are not fixed. The curvature given in Table 1 is only a candidate. There is the possibility that the other parameters were also slightly changed). The important differences between Advanced LIGO and LCGT are in the mirror curvature radius, beam radius, mirror material and temperature.

Table 1: Specification of Advanced LIGO [4, 5, 6] and LCGT [2].

	Advanced LIGO	LCGT
Laser beam profile	Gaussian	Gaussian
Wavelength	1064 nm	1064 nm
Cavity length	4000 m	3000 m
Front mirror curvature radius	2076 m	7114 m
End mirror curvature radius	2076 m	7114 m
Beam radius at the mirrors	60 mm	35 mm
Power in a cavity	0.83 MW	0.41 MW
Mirror material	Fused silica	Sapphire
Mirror mass	40 kg	30 kg
Mirror temperature	300 K	20 K

The upper limit of the strength of the parametric instability of LCGT is comparable with that of Advanced LIGO [7]. The number of the unstable modes is 10-times less than that of Advanced LIGO. The mirror curvature dependence of the instability strength (R) in the various elastic modes is weaker than that of Advanced LIGO. The strength R is not changed drastically by a shift of a few ten meters in the LCGT mirror curvature. It is easier to satisfy the requirement of the mirror curvature.

The difference in the parametric instabilities between Advanced LIGO and LCGT is caused by those of the beam radii (Advanced LIGO, 60 mm; LCGT, 35 mm) and the mirror materials (Advanced LIGO, fused silica; LCGT, sapphire). These differences mostly originate from that of the thermal noise-reduction methods (Advanced LIGO, fused silica mirrors with larger laser beams; LCGT, cooling sapphire mirrors), which are the main strategies of the projects.

The elastic Q reduction [8] by the barrel surface (0.2 mm thickness Ta_2O_5) coating is effective for the instability suppression in the LCGT arm cavity. In this case, Q-values are 10^6. The thermal noise of the barrel surface loss is a few times less than the goal sensitivity of LCGT.

3 Effect of PR and RSE

3.1 References about effect of PR and RSE

The PR effect is discussed in Ref. [9]. The parametric instability of an interferometer with PR and (detuned) signal recycling (SR) is investigated in Ref. [10]. The formulas in Ref. [10] are available for the case of RSE. In in Ref. [10], it is assumed that the optical transverse modes of both cavities are exactly same. On the other hand, in Ref. [11], the effect of the optical transverse mode difference in these two cavities is taken into account. In this report, mainly, the effects of PR and RSE techniques are studied using the formulas in Ref. [10]. The effect of the difference of the optical transverse modes in two cavities is shown shortly.

3.2 Formula with PR and RSE

The formula of the parametric instability of a Fabry-Perot cavity (without PR, RSE, and anti-Stokes modes) is derived in Ref. [1]. If a parameter R of an elastic mode is larger than unity, that mode is unstable. The formula of R is

$$R = \sum_{\text{optical mode}} \frac{4PQ_\mathrm{m}Q_\mathrm{o}}{McL{\omega_\mathrm{m}}^2} \frac{\Lambda_\mathrm{o}}{1+\Delta\omega^2/{\delta_\mathrm{o}}^2}, \tag{1}$$

where $P, Q_\mathrm{m}, Q_\mathrm{o}, M, c, L, \omega_\mathrm{m}, \Delta\omega$, and δ_o are the optical power in the cavity, the Q-values of the elastic and optical modes, the mass of the mirror, the speed of light, the cavity length, the angular frequency of the elastic mode, the angular frequency differences between the elastic and optical modes, and the half-width angular frequency of the optical mode, respectively. The value Λ_o represents the spatial overlap between the optical and elastic modes. If the shapes of the optical and elastic modes are similar, Λ_o is on the order of unity. If the shapes are not similar, Λ_o is almost zero. When the shapes and frequencies of the optical and elastic modes are similar ($\Lambda_\mathrm{o} \sim 1, \Delta\omega \sim 0$), R will become several thousands in future projects [9].

The formula with PR and RSE is described as [10]

$$R = \sum_{\text{optical mode}} \left(\frac{2PQ_\mathrm{m}Q_\mathrm{PR}}{McL{\omega_\mathrm{m}}^2} \frac{\Lambda_\mathrm{o}}{1+\Delta\omega^2/{\delta_\mathrm{PR}}^2} + \frac{2PQ_\mathrm{m}Q_\mathrm{RSE}}{McL{\omega_\mathrm{m}}^2} \frac{\Lambda_\mathrm{o}}{1+(\Delta\omega-\Delta_\mathrm{RSE})^2/{\delta_\mathrm{RSE}}^2} \right). \tag{2}$$

The first and second terms represent the effects of the PR and RSE, respectively. If there is no PR and RSE mirrors, each term is exactly same as the half of Eq. (1). Thus, in this case, Eq. (2) is equal to Eq. (1). The new parameters appear in Eq. (2). The factors Q_PR and Q_RSE are the optical Q-values of the arm cavity with the PR and RSE mirror.

They are written as

$$Q_{\rm PR} \sim Q_{\rm o}\frac{4}{T_{\rm PR}}, \tag{3}$$

$$Q_{\rm RSE} \sim Q_{\rm o}\frac{1}{T_{\rm RSE}}\left[\frac{{T_{\rm RSE}}^2}{4}+2\cos^2\phi\left(2-T_{\rm RSE}-\frac{{T_{\rm RSE}}^2}{4}\right)\right], \tag{4}$$

where $T_{\rm PR}, T_{\rm RSE}, \phi$ are the power transmittance of PR and RSE mirrors and phase advance between the RSE mirror and the beam splitter (if the tuned SR or RSE is adopted, ϕ is 0 or $\pi/2$ rad). The the half-width angular frequencies of the optical mode with PR and RSE are

$$\delta_{\rm PR} \sim \delta_{\rm o}\frac{T_{\rm PR}}{4}, \tag{5}$$

$$\delta_{\rm RSE} \sim \delta_{\rm o}\frac{T_{\rm RSE}}{\frac{{T_{\rm RSE}}^2}{4}+2\cos^2\phi\left(2-T_{\rm RSE}-\frac{{T_{\rm RSE}}^2}{4}\right)}. \tag{6}$$

In short, the PR and RSE mirrors change the effective finesse of the arm cavity. Especially, $4/T_{\rm PR}$ is equal to the power recycling gain. If the detuned RSE is adopted, the effective resonant frequency of the cavity changes. The $\Delta_{\rm RSE}$ in Eq. (2) corresponds to this resonant frequency shift:

$$\Delta_{\rm RSE} = \frac{\omega_{\rm o}}{2Q_{\rm o}}\frac{\sin 2\phi}{\frac{{T_{\rm RSE}}^2}{8}+\cos^2\phi\left(2-T_{\rm RSE}-\frac{{T_{\rm RSE}}^2}{4}\right)}. \tag{7}$$

The value $\omega_{\rm o}$ is the angular frequency of optical transverse mode.

3.3 Parametric instability of LCGT interferometer

The parameters of PR and RSE for LCGT are summarized in Table 2. In this article, the variable RSE in Ref. [12] is considered. In this section, it is assumed that $Q_{\rm m}$ is 10^8.

Table 2: Parameters of power recycling and RSE for LCGT [12].

$T_{\rm PR}$	0.37
$T_{\rm RSE}$	0.15
ϕ(tuned)	90 degree
ϕ(detune)	86.5 degree

The parameter $Q_{\rm PR}$ of LCGT is

$$Q_{\rm PR} \sim Q_{\rm o}\frac{4}{T_{\rm PR}} = 11Q_{\rm o}. \tag{8}$$

Therefore, the maximum of the power recycling term, the first term of Eq. (2), is 11/2=5.5 times larger than R of a cavity without PR and RSE in Eq. (1). Since the maximum R of a cavity is several hundreds [3], the maximum of the power recycling term is a few thousands. On the other hand, the peak width is

$$\frac{\delta_{\rm PR}}{2\pi} \sim \frac{\delta_{\rm o}}{2\pi}\frac{T_{\rm PR}}{4} = 16\,{\rm Hz} \times \frac{1}{11} = 1.5\,{\rm Hz}. \tag{9}$$

If the difference between the frequencies of the optical and elastic modes are much larger than 1.5 kHz, the power recycling term is smaller than R of a cavity in Eq. (1).

In the case of the tuned RSE, $Q_{\rm RSE}$ is

$$Q_{\rm RSE} \sim Q_{\rm o}\frac{T_{\rm RSE}}{4} = 0.038 Q_{\rm o}. \tag{10}$$

Therefore, the RSE term, the second term of Eq. (2), is 2/0.038=53 times smaller than R of a cavity in Eq. (1). Since the maximum R of a cavity is several hundreds [3], the maximum of the RSE term is a few tens. On the other hand, the peak width is

$$\frac{\delta_{\rm RSE}}{2\pi} \sim \frac{\delta_{\rm o}}{2\pi}\frac{4}{T_{\rm RSE}} = 16\,{\rm Hz} \times \frac{1}{0.038} = 430\,{\rm Hz}. \tag{11}$$

If the difference between the frequencies of the optical and elastic modes are much larger than 430 kHz, the RSE term is larger than R of a cavity in Eq. (1).

In the case of the detuned RSE, $Q_{\rm RSE}$ is

$$Q_{\rm RSE} \sim Q_{\rm o}\frac{1}{T_{\rm RSE}}\left[\frac{{T_{\rm RSE}}^2}{4} + 2\cos^2\phi\left(2 - T_{\rm RSE} - \frac{{T_{\rm RSE}}^2}{4}\right)\right] = 0.13 Q_{\rm o}. \tag{12}$$

Therefore, the RSE term, the second term of Eq. (2), is 2/0.13=15 times smaller than R of a cavity in Eq. (1). Since the maximum R of a cavity is several hundreds [3], the maximum of the RSE term is a several tens. On the other hand, the peak width is

$$\delta_{\rm RSE} \sim \delta_{\rm o}\frac{T_{\rm RSE}}{\frac{{T_{\rm RSE}}^2}{4} + 2\cos^2\phi\left(2 - T_{\rm RSE} - \frac{{T_{\rm RSE}}^2}{4}\right)} = 120\,{\rm Hz}. \tag{13}$$

The frequency shift by detune is

$$\frac{\Delta_{\rm RSE}}{2\pi} = \frac{1}{2\pi}\frac{\omega_{\rm o}}{2Q_{\rm o}}\frac{\sin 2\phi}{\frac{{T_{\rm RSE}}^2}{8} + \cos^2\phi\left(2 - T_{\rm RSE} - \frac{{T_{\rm RSE}}^2}{4}\right)} = 200\,{\rm Hz}. \tag{14}$$

3.4 Effect of difference between arm cavities

If the frequency difference between optical transverse modes of both arm cavities are larger than $\Delta_{\rm RSE}$, this difference must be taken into account [11]. In this case, the effect of PR and RSE (the first and second terms in Eq. (2)) mix with each other. Although the peak height of the effect of RSE (the second term in Eq. (2)) is not so changed

by this mixing, the peak height of the effect of PR (the first term in Eq. (2)) becomes comparable with the RSE peak height. This is a similar phenomenon as follows. When two oscillators which have similar resonant frequencies but extremely different Q-values are coupled, both Q-values of the new two modes are comparable with smaller original one. In short, the maximum of the parametric instability becomes smaller when the frequency difference between optical transverse modes of both arm cavities is large. As described in next section, the parametric instability is perfectly suppressed in such a case. It is not necessary to consider this difference seriously.

4 Instability suppression with PR and RSE

The investigation without PR and RSE [3] revealed that the loss coating on the barrel surfaces of the mirrors is the effective method to suppress the parametric instability. If the Q-values of the mirrors with the barrel surface loss are 10^6, almost all modes are stable. The thermal noise caused by this barrel surface loss is a few times smaller than the goal sensitivity of LCGT.

Figure 1 shows that the maximum R in the various elastic modes in the LCGT interferometer when the mirror Q values with the barrel surface loss are 10^6. The solid and dashed lines show the maximum R with and without [3] PR and RSE. The RSE term, the second one in Eq. (2), does not appear in Fig. 1 because the maximum value is smaller than unity if $Q_{\rm m}$ is 10^6 (in the previous section, $Q_{\rm m}$ is 10^8). Therefore, the details of RSE do not affect the parametric instability (if detune, which is a difference between 90 degree and ϕ, is not so large). The power recycling term, the first one in Eq. (2), has a higher peak. The width of the peak is narrower. Two new small peaks appear around 7100 m in Fig. 2. Since the thermal noise caused by the barrel surface loss is a few times smaller than the goal sensitivity, it is possible to make the Q-values a few times smaller. In short, all modes except for the highest peaks around 7050 m could disappear in Fig. 1. The details of the barrel surface loss must be considered.

5 Contribution of higher modes (preliminary result)

In this report, only elastic modes below 100 kHz and the first three optical transverse modes are considered. Here, preliminary results about contributions of higher modes with PR and PSE are summarized. Elastic modes between 100 kHz and 200 kHz are considered. However, only the first three optical transverse modes are taken into account. The elastic modes between 150 kHz and 200 kHz are always stable if Q values are 10^6. In short, they never appear in Fig. 1. It is expected that elastic modes above 200 kHz never become problems because Eq. (2) shows that a contribution for R of a higher mode is smaller.

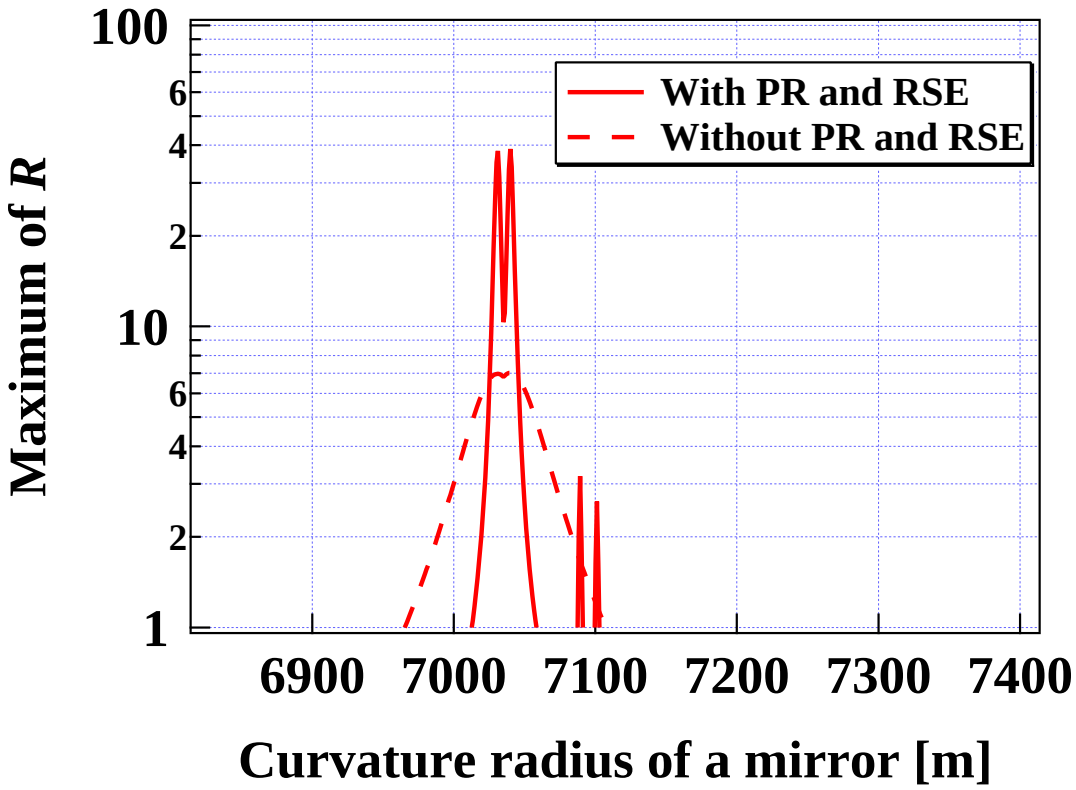

Figure 1: Maximum of R in the various elastic modes in the LCGT interferometer. The horizontal axis is the curvature radius of one mirror in both cavities. The curvature of the other mirrors is the default values given in Table 1. The Q-values of mirrors with barrel surface loss are 10^6. The solid and dashed lines are maximum R with and without [3] PR and RSE. If the maximum R is smaller than unity, all modes are stable.

However, peaks of about 10 modes between 100 kHz and 150 kHz appear in Fig. 1. They are unstable even if Q-values are 10^6. The maximum R of such modes is 4 at most. Since the thermal noise caused by the barrel surface loss is a few times smaller than the goal sensitivity, it is possible to make Q-values a few times smaller. All modes except for the highest peaks around 7050 m in Fig. 1 could disappear. The details of the barrel surface loss must be considered.

6 Contribution of anti-Stokes modes

Parametric instability occurs if the frequency of the optical transverse mode is lower than the carrier frequency (Stokes mode). On the other hand, if the optical transverse mode is higher than the carrier frequency (anti-Stokes), the optical and elastic modes suppress each other. In short, instabilities do not occur [13]. If the optical mode density is high,

anti-Stokes modes cancel Stokes modes. However, anti-Stokes modes do not so effectively decrease the parametric instability in Advanced LIGO [9]. Since the optical mode density of LCGT is smaller than that of Advanced LIGO, the anti-Stokes mode effect is not considered in this report.

7 Summary

The parametric instability of a LCGT arm cavity has already been investigated. Here, the parametric instability of the LCGT interferometer with the power recycling (PR) and resonant sideband extraction (RSE) is considered. Even PR and RSE are taken into account, the loss coating on the mirror barrel surfaces is the effective method to suppress the parametric instability. If the Q-values of the mirrors with the barrel surface loss are 10^6 (0.2 mm thickness Ta_2O_5), almost all modes are stable. Since detune of RSE is not so strong, the parametric instability is independent of details of RSE in the case of LCGT. The PR enhances the maximum of the instability strength R and decreases the width of peaks of R. Even if the contributions of higher modes are taken into account, it seems to be possible to make almost all mode stable. However, the further consideration is necessary.

References

[1] V.B. Braginsky *et al.*, Phys. Lett. A **287** (2001) 331.

[2] K. Kuroda *et al.*, Prog. Theor. Phys. Suppl. **163** (2006) 54.

[3] K. Yamamoto *et al.*, J. Phys.: Conf. Ser. **122** (2008) 012015.

[4] L. Ju *te al.*, Phys. Lett. A **354** (2006) 360.

[5] L. Ju *te al.*, Phys. Lett. A **355** (2006) 419.

[6] C. Zhao *et al.*, Phys. Rev. Lett. **94** (2005) 121102.

[7] P. Fritschel, in *Proceedings of the SPIE meeting Gravitational-Wave Detection (4856-39), Waikoloa, Hawaii, 2002*, edited by P. Saulson and M. Cruise (International Society for Optical Engineering, Washington, 2002),p. 282.

[8] S. Gras S *et al.*, J. Phys.: Conf. Ser. **32** (2006) 251.

[9] Braginsky V B, Strigin S E and Vyatchanin S P 2002 *Phys. Lett.* A **305** 111.

[10] Gurkovsky A G, Strigin S E and Vyatchanin S P 2007 *Phys. Lett.* A **362** 91.

[11] Strigin S E and Vyatchanin S P 2007 *Phys. Lett.* A **365** 10.

[12] LCGT special working group, Study report on LCGT interferometer observation band (September 8, 2009).

[13] Kells W and D'Ambrosio E 2002 *Phys. Lett.* A **299** 326